Supplementary Materials

Contents:

Supplemental Table S1. Molecular weight of the mammalian p53TD

Peptides	Calculated* ($M+H^+$)	Observed**
Human	4190.7	4190.8
Tree shrew	4231.8	4233.6
Guinea pig	4245.8	4245.9
Chinese hamster	4100.7	4100.7
Sheep	4220.8	4220.9
Opossum	4305.9	4305.9

*The calculated MH^+ (average) values were calculated by the protein prospector website at UCSF.
**The observed MH^+ molecular weights of the peptides were measured using MALDI-TOF MS (linear, positive mode).

Supplemental Table S2 Data collection and refinement statistics for p53TDs

Dataset	HU-p53TD	OP-p53TD	TS-p53TD
Data Collection			
Beamline	ID7B2, CHESS	ID7B2, CHESS	ID7B2, CHESS
Wavelength (Å)	0.9686	1.0000	1.0000
Space group	P 21 21 21	P 21 21 21	C 2 2 2
Unit cell parameters			
a, b, c (Å)	30.973, 56.437, 61.656	38.275, 50.887, 60.240	62.871, 65.806, 32.511
α, β, γ (°)	90, 90, 90	90 90 90	90 90 90
Resolution range (Å)	41.63 – 1.22 (1.264 – 1.22)	32.31 – 1.35 (1.398 – 1.35)	45.46 - 1.16 (1.201 - 1.16)
No. of unique reflections	30235 (1953)	24100 (1080)	21822 (1027)
Multiplicity	5.5 (2.4)	5.6 (1.9)	9.9 (2.8)
Completeness (%)	91.77 (60.35)	90.51 (39.14)	91.70 (43.72)
R_{merge}	0.04487 (0.2466)	0.08437(.9251)	0.04206 (0.3908)
CC_{merge}	1.0 (0.959)	0.999 (0.662)	1.0 (0.84)
I/σ(I)	19.68 (2.06)	12.46 (0.51)	28.35 (1.62)
Refinement Statistics			
Resolution (Å)	41.63 – 1.22	32.31 – 1.35	45.46 - 1.16
Reflections (total/test)[a]	30234 (1992)	24002 (1992)	21817 (2001)
R_{work}/R_{free} (%)	0.1464/0.1764	0.1711/0.2025	0.1736/0.1915
CC_{work}	0.967 (0.937)	0.964 (0.474)	0.947 (0.891)
CC_{free}	0.967 (0.804)	0.956 (0.395)	0.942 (0.861)
No. of atoms (excluding hydrogens)			
Protein	1155	1107	536
Water	147	133	99
B factors			
Protein	16.87	21.59	16.55
Water	29.03	32.73	28.90
Root-mean-square deviation			
Bond length (Å)	0.022	0.011	0.009
Bond angle (°)	1.74	1.11	1.09
Ramachandran (%)[b]			
Favored	98.39	100.00	100.00
Outliers	0.00	0.00	0.00

Values in parentheses are for highest-resolution shell. $\mathbf{R_{sym}} = \sum \mathbf{hkl} \sum \mathbf{i} |\mathbf{I_{hkl,i}} - \langle \mathbf{Ihkl} \rangle|$, where $\mathbf{I_{hkl,i}}$ is the intensity of an individual measurement of the reflection with Miller indices **hkl** and $\mathbf{I_{hkl}}$ is the mean intensity of the reflection. $\mathbf{R_{work}} = \sum \mathbf{hkl} ||\mathbf{F_o}| - |\mathbf{F_c}|| / \sum \mathbf{hkl} |\mathbf{F_o}|$, where $|\mathbf{F_o}|$ is the observed structure-factor amplitude and $|\mathbf{F_c}|$ is the calculated structure-factor amplitude. $\mathbf{R_{free}}$ is the R factor based on at least 500 test reflections that were excluded from the refinements. CLS (Canadian Light Source) and CHESS (Cornell High Energy Synchrotron Source).

[a] Reflection for $F_o > 0$. [b] MolProbity analysis.

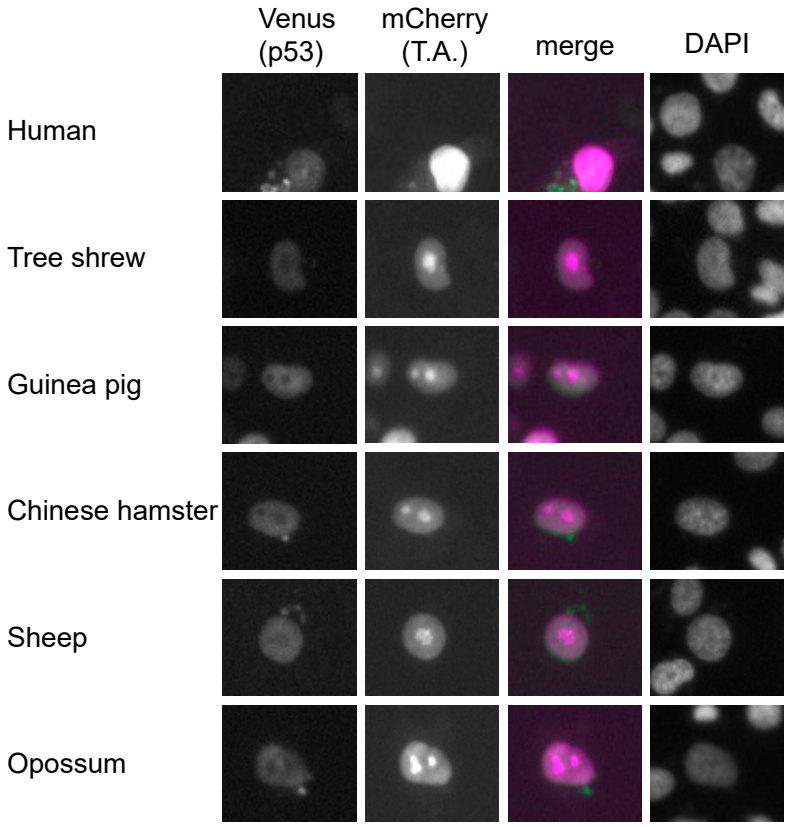

Supplemental Figure S1: Fluorescence images of the reporter assay. Chimeric p53 protein (Venus), p53-dependent transcriptional activity (mCherry), merged images of Venus (green) and mCherry (magenta), and DAPI staining were shown.

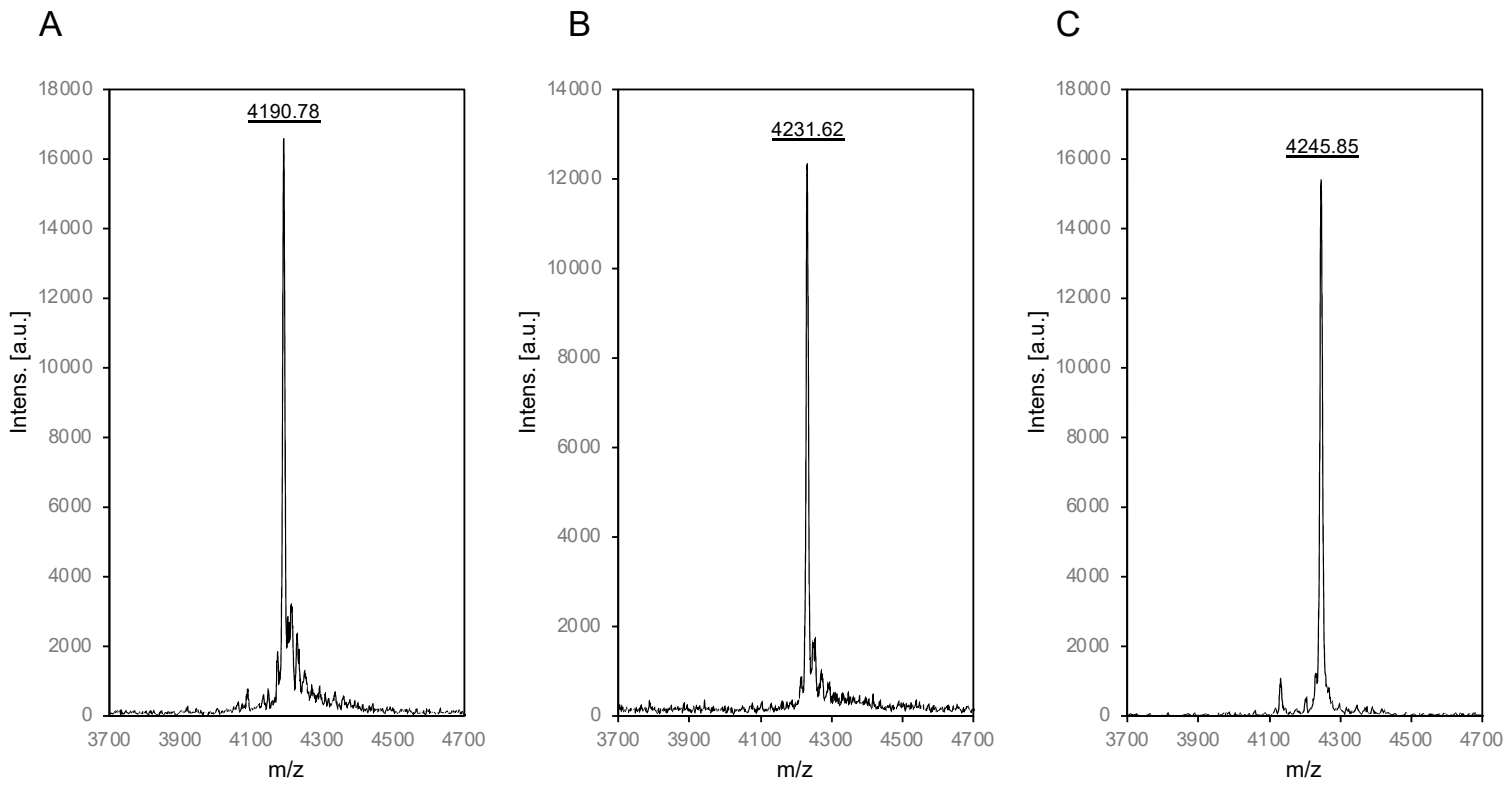

Supplemental Figure S2. MALDI-TOF MS spectra of the synthesized mammalian p53TD peptides. (A) Human, (B) Tree shrew, (C) Guinea pig, (D) Chinese hamster, (E) Sheep, (F) Opossum

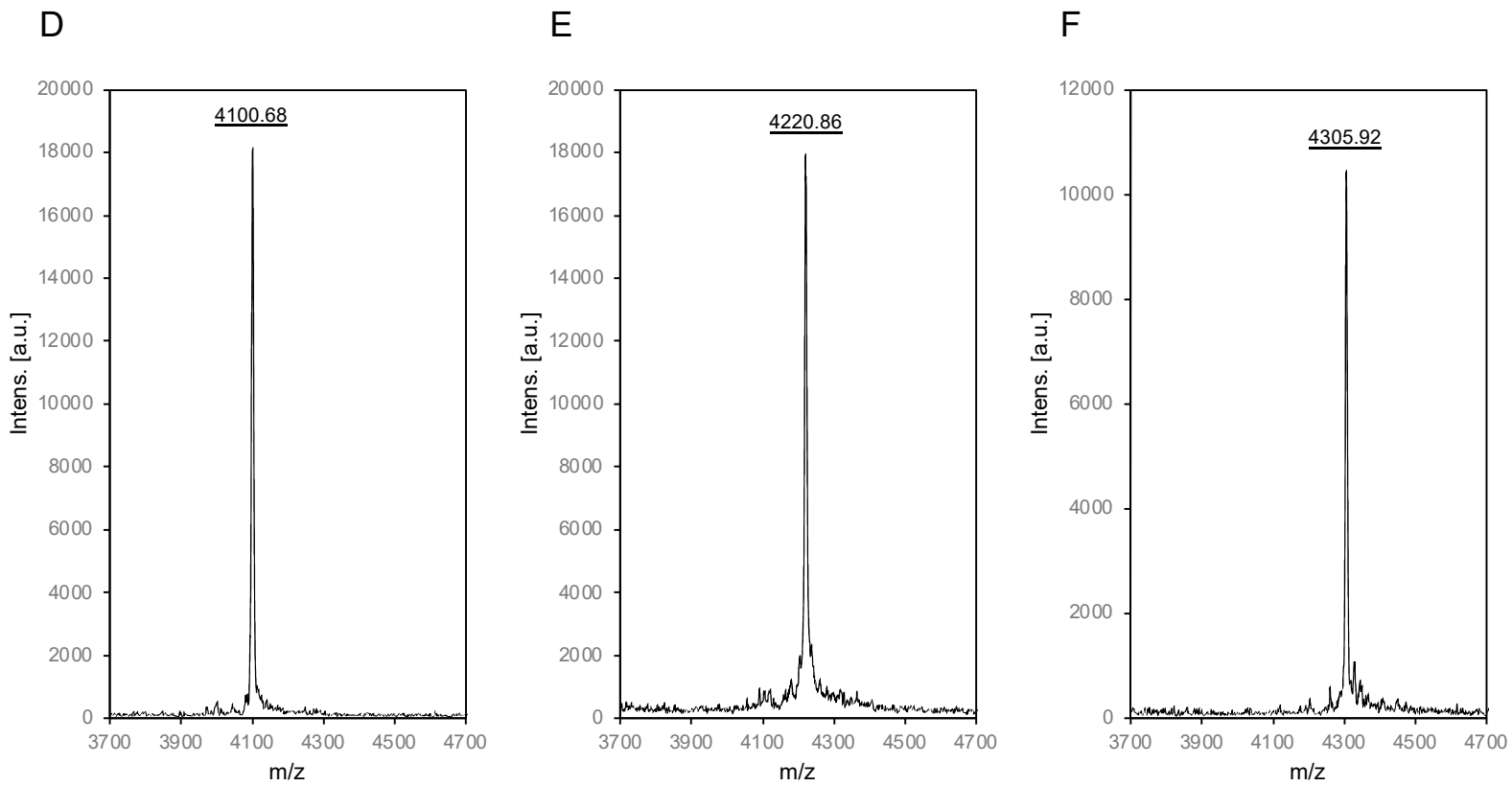

Supplemental Figure S2. MALDI-TOF MS spectra of the synthesized mammalian p53TD peptides. (A) Human, (B) Tree shrew, (C) Guinea pig, (D) Chinese hamster, (E) Sheep, (F) Opossum

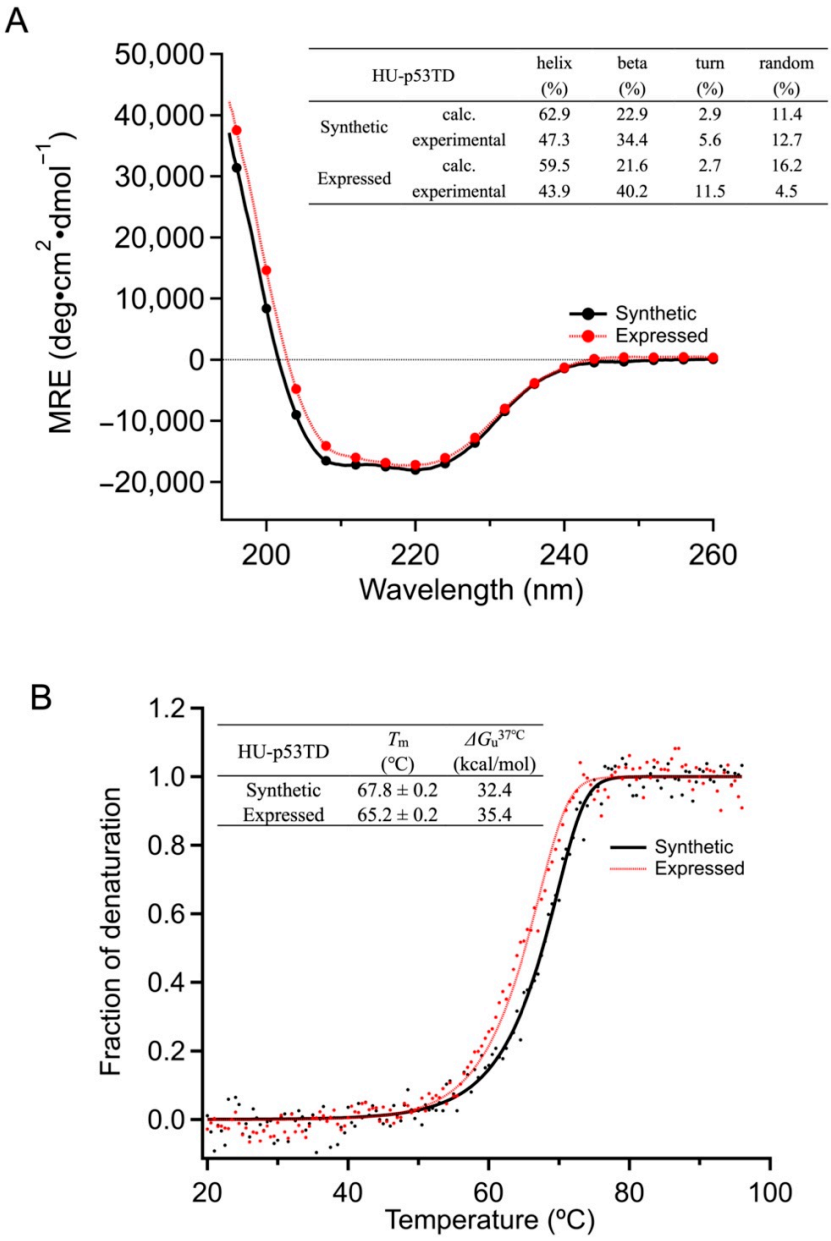

HU-p53TD		helix (%)	beta (%)	turn (%)	random (%)
Synthetic	calc.	62.9	22.9	2.9	11.4
	experimental	47.3	34.4	5.6	12.7
Expressed	calc.	59.5	21.6	2.7	16.2
	experimental	43.9	40.2	11.5	4.5

HU-p53TD	T_m (°C)	$\Delta G_u^{37°C}$ (kcal/mol)
Synthetic	67.8 ± 0.2	32.4
Expressed	65.2 ± 0.2	35.4

Supplemental Figure S3. CD spectra (A) and thermal denaturation curves of the synthetic and the expressed HU-p53TD peptides. (A) The secondary structure of the HU-p53TD peptides were measured by CD spectrometry at 4°C. The percentage of secondary structural elements were calculated. (B) The signals from the HU-p53TDs (synthetic and expressed in *E.coli*) were monitored by CD spectrometry at 222 nm between 4°C and 96°C. The fraction of denaturation at each temperature was plotted to generate the denaturation curves.

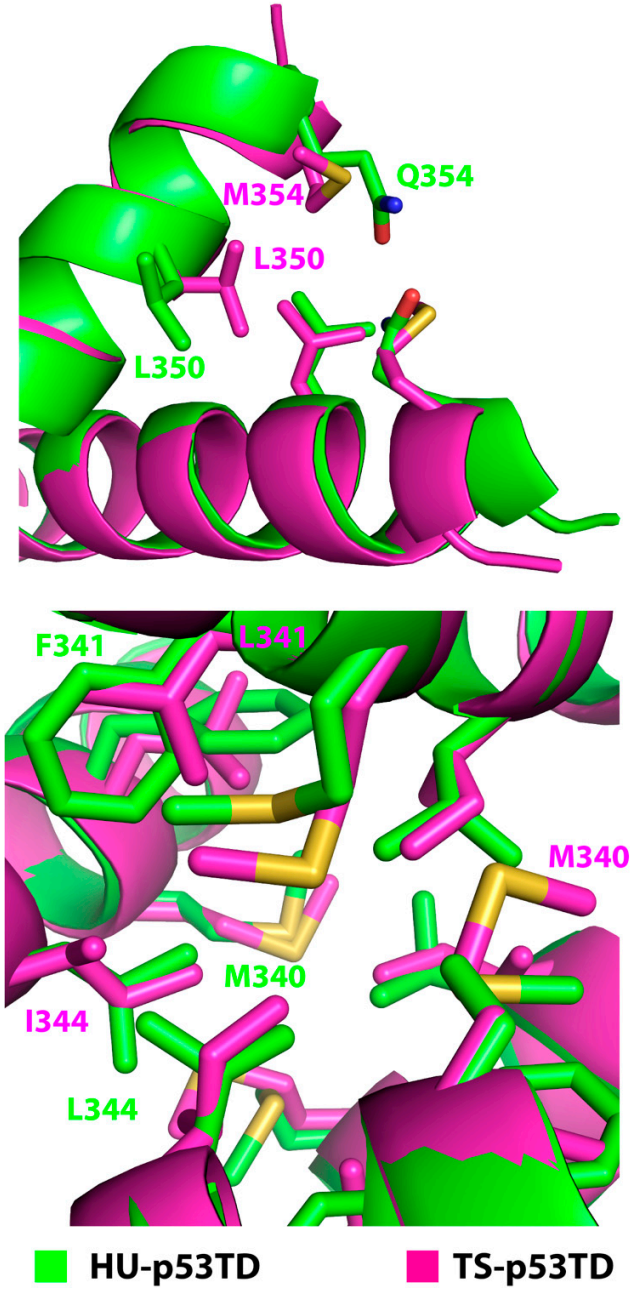

Supplemental Figure S4. Overlay of the regions containing the key structural differences between the HU-p53TD (green) and the TS-p53TD (Magenta). The upper panel shows a zoom of the C-terminal end of the α-helix highlighting the side chains of residues L350 and Q354 of HU-p53TD (green) and the corresponding L350 and M354 of TS-p53TD (magenta). The lower panel shows the zoom of the central region of the α-helix highlighting the side chains of residues M340, F341 and L344 of HU-p53TD (green) and the corresponding M340, L341 and I344 of TS-p53TD (magenta).

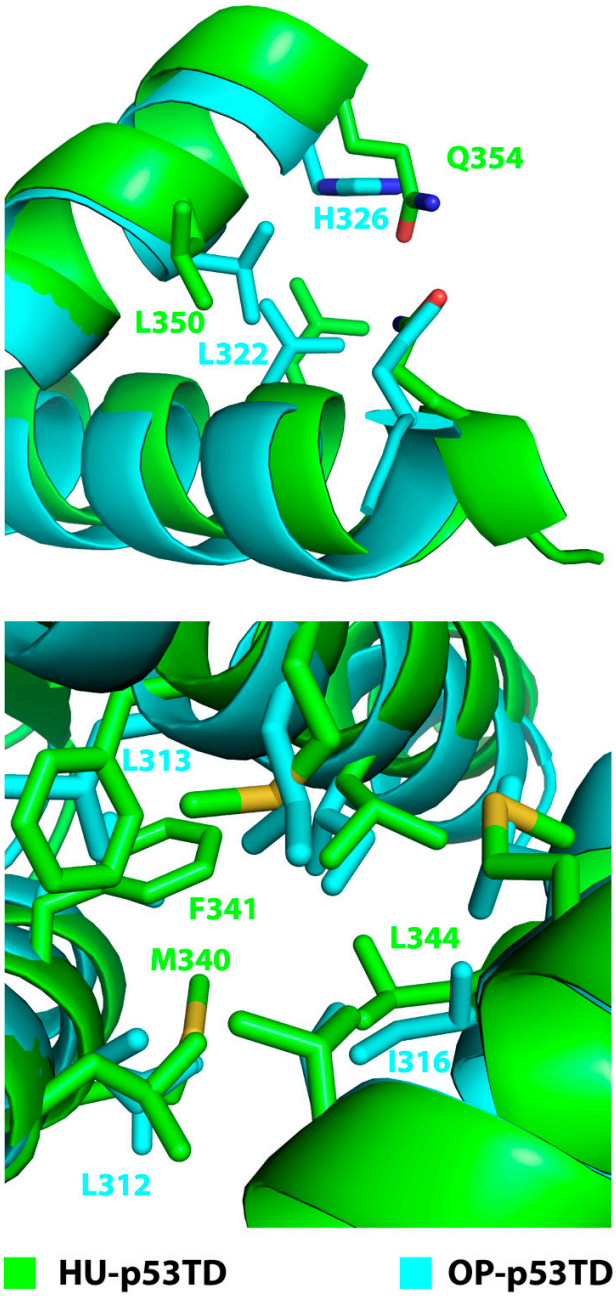

Supplemental Figure S5. Overlay of the regions containing the key structural differences between the HU-p53TD (Green) and the OP-p53TD (Aqua). The upper panel shows a zoom of the C-terminal end of the α-helix highlighting the side chains of residues L350 and Q354 of HU-p53TD (Green) and the corresponding L322 and H326 of OP-p53TD (Aqua). The lower panel shows the zoom of the central region of the α-helix highlighting the side chains of residues M340, F341 and L344 of HU-p53TD (Green) and the corresponding L312, L313 and I316 of OP-p53TD (Aqua)